JACS
JOURNAL OF THE AMERICAN CHEMICAL SOCIETY
Communication
Cite This: J. Am. Chem. Soc. 2019, 141, 20048−20052
pubs.acs.org/JACS

Total Synthesis of (−)-Oridonin: An Interrupted Nazarov Approach

Lingran Kong,[†,§] Fan Su,[†,§] Hang Yu,[†] Zhe Jiang,[†] Yandong Lu,[†] and Tuoping Luo*[,†,‡]

[†]Key Laboratory of Bioorganic Chemistry and Molecular Engineering, Ministry of Education and Beijing National Laboratory for Molecular Science, College of Chemistry and Molecular Engineering, Peking University, Beijing 100871, China

[‡]Peking-Tsinghua Center for Life Sciences, Academy for Advanced Interdisciplinary Studies, Peking University, Beijing 100871, China

Supporting Information

ABSTRACT: An enantioselective total synthesis of (−)-oridonin is accomplished based on a key interrupted Nazarov reaction. The stereochemistry of the Nazarov/Hosomi−Sakurai cascade was first explored to forge a tetracyclic skeleton with challenging quaternary carbons. A delicate sequence of two ring-rearrangements and late-stage redox manipulations was carried out to achieve the de novo synthesis of this highly oxidized *ent*-kauranoid.

Among over 1000 *ent*-kaurene diterpenoids that are biosynthetically related to *ent*-kaurene (Figure 1, **1**),[1]

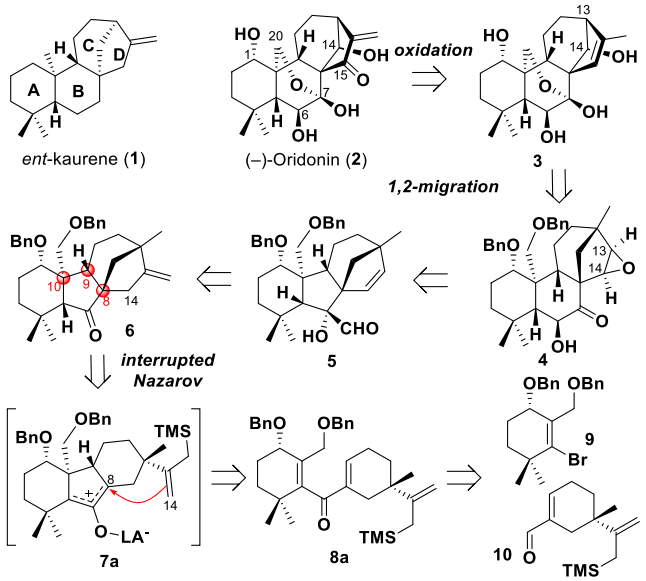

Figure 1. (−)-Oridonin (**2**) and its retrosynthetic analysis.

(−)-oridonin (**2**) is one of the most widely used and investigated members in both the clinical and preclinical settings.[2] As a matter of fact, it is the major active ingredient of *Rabdosia rubescens*, an over-the-counter anti-inflammatory herbal medicine commonly available in China.[2b] The promising activities of **2** against a wide variety of cancer cells in vitro and in vivo prompted intensive medicinal chemistry efforts via semisynthesis, leading to a series of oridonin derivatives to fine-tune its properties for drug development.[3] Among them, HAO472 has recently entered the phase I clinical trial in China for the treatment of acute myelogenous leukemia.[4] Furthermore, recent researches have also piqued interest in the potential of **2** in the area of neuroprotection and neurodegenerative diseases.[5] In terms of the mechanism-of-action studies, a number of target proteins have been identified to react with the α-methylene cyclopentanone unit of **2**, including oncoprotein AML1-ETO, and NLRP3, the central component of the NLRP3 inflammasome.[6]

Although semisynthesis of oridonin has been achieved[7] and significant progress has been made in the chemical synthesis of *ent*-kaurenoids with high oxidation level,[8−10] oridonin (**2**) still presents a daunting task for total synthesis, inviting the development of new and effective synthetic strategies given its unique structural features. To illustrate, attempts to access **2** via our previous approach that accomplished maoecrystal P was hampered by the presence of a C14 hydroxyl group.[9d] Considering that subtle structural differences have tremendous impacts on the biological activities within this family of natural products, we embraced the development of a de novo synthesis of (−)-oridonin (**2**) that would open the opportunity for flexible and deep-seated structural changes inaccessible by semisynthesis. Herein, we report our efforts leading to the total synthesis of (−)-oridonin (**2**).

Our retrosynthetic analysis commenced with the recognition that the late-stage intermediate **3** could be prepared from epoxide **4** via 1,2-migration and deprotection.[11] Another 1,2-migration (acyloin rearrangement) was devised to trace **4** back to **5**, inspired by the conversion of gibberellic acid to kaurenoids reported by the Mander group.[12] This strategic ring contraction revealed a key synthetic intermediate (**6**) that contained two quaternary carbons, C8 and C10 (oridonin numbering, throughout), and one tertiary stereogenic center without neighboring controlling functional groups, C9. We envisaged an interrupted Nazarov cyclization that trapped oxyallyl cation **7a** using a pendant allylsilane for the efficient synthesis of **6**.[13,14] Consequently, the substrate of this key reaction, ketone **8a**, could be prepared by two monocyclic synthons, **9** and **10**. The grand challenge of our plan was the feasibility and efficiency of the Nazarov/Hosomi−Sakurai cascade, even if the disconnection of the C8−C14 bond via a positive charge and an allylsilane moiety was reminiscent of the maoecrystal V synthesis reported by Baran's group.[10i] Furthermore, we anticipated significant experimentations

Received: November 7, 2019
Published: December 5, 2019

DOI: 10.1021/jacs.9b12034
J. Am. Chem. Soc. 2019, 141, 20048−20052

would be required to resolve the challenges presented by not only the ring rearrangements but also late-stage functional group manipulations on such a strained, highly oxidized, and sterically hindered polycyclic skeleton.

The influence of the stereochemistry (C1 and C16) on the proposed Nazarov/Hosomi–Sakurai cascade was first evaluated, which turned out to be of paramount importance (Table 1 and Table S1). The substrate, ketone **8**, was prepared as a diastereomeric mixture of 1:1 ratio (Scheme S1). Screening of various Lewis acids only led to decomposition or desilylation products, whereas only $EtAlCl_2$ facilitated the desired transformation and therefore was used for subsequent optimizations. The identifiable products (**11**–**14**) revealed two important features of this reaction: (1) the torquoselectivity could be rationalized by the presence of C1 and C20 OBn groups, which led to different steric interactions between the two possible conrotatory pathways (**A**); (2) the formation of the interrupted versus normal Nazarov products was achieved in a stereoselective fashion. The π-nucleophile, allylsilane, smoothly approached C8 anti to the adjacent C9 hydrogen (**8b**); in contrast, the rate of proton elimination outcompeted the interception of the oxyallyl cation generated from enone **8a**. In terms of the reaction condition optimization, dramatic solvent effects were discovered: while both dichloromethane (DCM) and acetonitrile provided products **11** and **12** in the presence of a catalytic amount of $EtAlCl_2$, tetrahydrofuran (THF) completely inhibited the reaction (Table 1, entries 1–3, and Table S1). However, scale-up of the reaction using DCM as the solvent led to a deteriorated and unstable yield of **11** (entry 4), and scale-up of the reaction in acetonitrile resulted in the formation of side product **13**, which was hard to separate from desired **11** (entry 5). The problem was solved by employing solvent mixture (DCM/THF = 20:1) with increased equivalents of $EtAlCl_2$, which robustly afforded **11** and **14** in >30% and >20% yield, respectively (entries 6 and 7).

Based on the study of the Nazarov/Hosomi–Sakurai cascade, we revised our synthetic plan to prepare (+)-**9** (Scheme 1). β-Bromo aldehyde **16** provided by Vilsmeier reaction[15] of ketone **15** was first converted to ester **17** via Pinnick oxidation and methylation. By screening a variety of allylic oxidation conditions, we found CrO_3 could provide enone **18** with a yield of 45% on a 20 g scale,[16] whereas remaining **17** (33%) was readily separated and recycled. By adding excess BMS (borane dimethyl sulfide complex), CBS (2-methyl-CBS-oxazaborolidine) reduction of **18** directly afforded chiral diol (+)-**19** in excellent enantioselectivity (>98% ee),[17] which was protected by a benzyl group to yield (+)-**9**. On the other hand, we commenced the synthesis of the right-wing fragment (**10**) from (+)-**20**, the enantiomer of which was prepared in high enantiopurity by Hoveyda's group.[18] For practical reasons, we further optimized the enantioselective 1,4-addition with reduced catalyst loadings during the scale-up, resulting in a protocol that provided (+)-**20** in 86% ee on a multigram scale (see SI). Ketone **20** was converted to vinyl iodide **21** upon treatment with ICl (iodine monochloride),[19] followed by the Pd-catalyzed cross-coupling with trimethylsilylmethylzinc reagent to give allylsilane **22** in 55% yield over two steps.[20] Regioselective deprotonation of the less sterically hindered α-methylene of the carbonyl group in **22** led to an enol triflate that underwent Pd-catalyzed

Table 1. Optimization of the Interrupted Nazarov Reaction

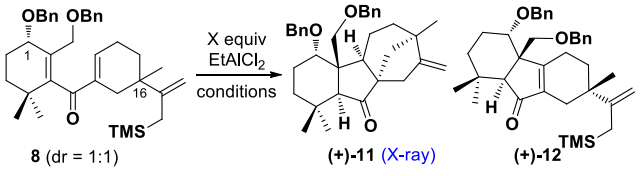

8a: R^1 = -$C(CH_2)CH_2TMS$, R^2 = -Me
8b: R^1 = -Me, R^2 = -$C(CH_2)CH_2TMS$

			yield (%)[a]			
entry	X	conditions	11	12	13	14
1	0.3	DCM, 40 °C, 2 h[b]	24	13	0	0
2	2	THF, 40 °C, 24 h[b,c]	0	0	0	0
3	0.35	MeCN, 40 °C, 8 h[b]	15	27	0	0
4	0.3	DCM, 40 °C, 1 h[d]	23	nd	0	0
5	0.35	MeCN, 40 °C, 8 h[d]	20	43	10	0
6	1.5	DCM/THF = 20:1, 40 °C, 24 h[d]	32	0	0	20
7	1.5	DCM/THF = 20:1, 40 °C, 24 h[e]	35	0	0	21

[a]Isolated yield after flash chromatography. [b][**8**] = 0.05 M (0.04 mmol). [c]Substrate **8** was recovered. [d][**8**] = 0.05 M (0.4 mmol). [e][**8**] = 0.1 M (2 g scale).

Scheme 1. Preparation of Fragments (+)-9 and (+)-10[a]

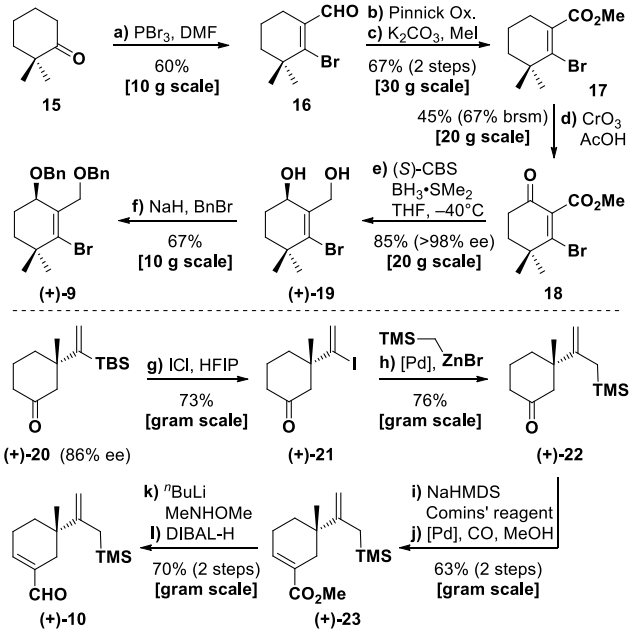

[a]Reagents and conditions: (a) PBr_3, DMF, $CHCl_3$, 0 to 70 °C, 60%; (b) NaH_2PO_4, H_2O_2, $NaClO_2$, CH_3CN/H_2O, 0 to 30 °C; (c) K_2CO_3, CH_3I, DMF, rt, 67% (2 steps); (d) CrO_3, AcOH, Ac_2O, DCM, rt, 45%, 67% brsm; (e) (*S*)-oxazaborolidine (0.60 equiv), $BH_3{\cdot}SMe_2$ (1.6 equiv), THF, 0 °C, then **18**, −40 °C, 85%; (f) NaH, BnBr, THF, 30 °C, 67%; (g) ICl, diglyme, HFIP, 40 °C, 73%; (h) $Pd(MeCN)_2Cl_2$ (0.1 equiv), $TMSCH_2ZnBr$, DMF, 45 °C, 76%; (i) NaHMDS, diglyme, then Comins' reagent, ^{t}BuOMe, −78 °C; (j) $Pd(OAc)_2$ (0.12 equiv), PPh_3 (0.24 equiv), CO, Et_3N, DMF/MeOH, 45 °C, 63% (2 steps); (j) $CH_3NHOCH_3{\cdot}HCl$, ^{n}BuLi, THF, −78 °C; (e) DIBAL-H, THF, −78 °C, 70% (2 steps).

DOI: 10.1021/jacs.9b12034
J. Am. Chem. Soc. 2019, 141, 20048–20052

Scheme 2. Total Synthesis of (−)-Oridonin (2)[a]

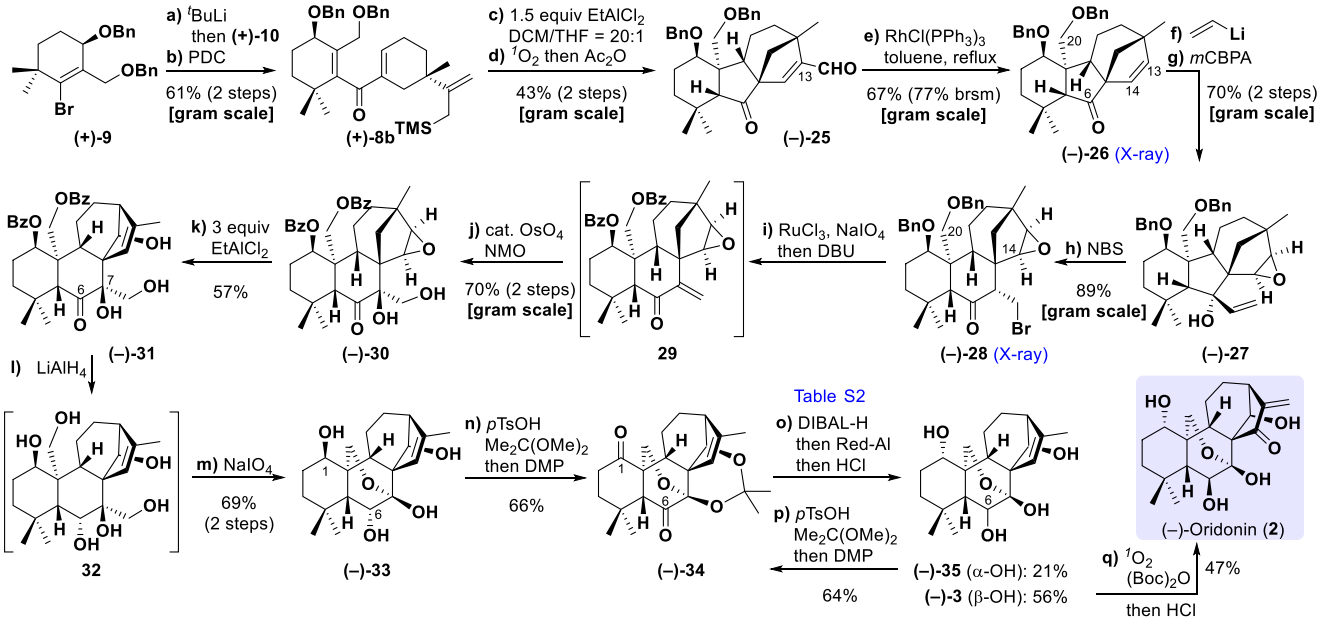

[a]Reagents and conditions: (a) ^{t}BuLi, Et_2O, −78 °C, then (+)-**10**; (b) PDC, DMF, 0 °C to rt, 61% (2 steps); (c) $EtAlCl_2$, DCM/THF = 20:1, 40 °C; (d) TPP, O_2, $CDCl_3$, rt, then Ac_2O, pyridine, DMAP, rt, 43% (2 steps); (e) $RhCl(PPh_3)_3$, toluene, reflux, 67%, 77% brsm; (f) vinyl bromide, ^{t}BuLi, − 78 °C, then (−)-**26**, 0 °C; (g) *m*CPBA, $NaHCO_3$, DCM, 0 °C, 70% (2 steps); (h) NBS, DCM, rt, 89%; (i) $RuCl_3{\cdot}3H_2O$, $NaIO_4$, CH_3CN/CCl_4, 0.2 M buffer, rt, then DBU; (j) OsO_4, NMO, acetone/H_2O, 40 °C, 70% (2 steps); (k) $EtAlCl_2$, toluene, 0 °C to rt, 57%; (l) $LiAlH_4$, Et_2O, rt; (m) $NaIO_4$, THF/buffer, 10 °C to rt, 69% (2 steps); (n) *p*TsOH, 2,2-dimethoxypropane, acetone, rt, then $NaHCO_3$, DMP, DCM, 0 °C to rt, 66%; (o) DIBAL-H, DCM/ether, −100 °C to rt, then Red-Al, rt, then HCl(aq) **35**, 21%; **3**, 56%; (p) *p*TsOH, 2,2-dimethoxypropane, acetone, rt, then $NaHCO_3$, DMP, DCM, 0 °C to rt, 64%; (q) TPP, O_2, $CDCl_3$, rt, then $(Boc)_2O$, pyridine, DMAP, DCM, 0 °C, then HCl(aq), dioxane, 47%. PDC, pyridinium dichromate; TPP, 5,10,15,20-tetraphenylporphin; *m*CPBA, *m*-chloroperoxybenzoic acid; NBS, *N*-bromosuccinimide; DBU, 1,8-diazabicyclo[5.4.0]undec-7-ene; DMP, Dess−Martin periodinane; NMO, 4-methylmorpholine *N*-oxide.

carbonylation to give ester **23** in 63% yield over two steps. Converting **23** to Weinreb amide **24** followed by diisobutylaluminum hydride (DIBAL-H) reduction provided enantioenriched aldehyde (+)-**10**.

With two abundant fragments in hand, we moved on to the total synthesis of (−)-oridonin (**2**) (Scheme 2). The addition of (+)-**10** to the lithium reagent prepared by Li−Br exchange of (+)-**9** with ^{t}BuLi afforded a pair of diastereomeric secondary alcohols, which were oxidized by pyridinium dichromate (PDC) to furnish (+)-**8b** in 61% yield over two steps. Under the optimized conditions of the Nazarov/Hosomi−Sakurai cascade, (+)-**8b** was converted to (−)-**11**, the crude product of which was directly subjected to singlet oxygen ene reaction followed by acetate anhydride treatment to afford aldehyde (−)-**25** in 43% yield over two steps.[21] The cleavage of an extra carbon on C13 was realized by the subsequent rhodium-catalyzed deformylation,[22] providing ketone **26** in 67% yield on a gram scale. The blockage of the *re* face of the C6 carbonyl group by the C20 substituent was evident in the X-ray structure of **26**, whereas we only accomplished the 1,2-addition by vinyl lithium after screening various nucleophilic reagents, and the resulting alcohol was selectively epoxidized by *m*-chloroperbenzoic acid (*m*CPBA) on the C13−C14 olefin to give **27** as a single diastereomer in 70% yield over two steps. Attempts to oxidatively cleave the vinyl group in **27** to an aldehyde all met with failure, presumably due to the insurmountable steric hindrance and the high oxidation level of the substrate. Eventually, a pinacol-like rearrangement forged the B ring by introducing an electrophilic bromine to the carbon−carbon double bond, leading to **28** as a single diastereomer in 89% yield on a gram scale,[23] the structure of which was determined unambiguously by X-ray diffraction. To avoid the opening of epoxide by C20−OBn under Lewis acid conditions, as well as side reactions associated with the labile bromide, we first carried out a series of oxidative transformations on **28**. Conversion of two benzyl protecting groups to benzoyl ones was followed by treatment of 1,8-diazabicyclo[5.4.0]undec-7-ene (DBU) to deliver enone **29**,[24] and subsequent dihydroxylation afforded **30** in 70% yield over two steps. Among the Lewis acids evaluated, $EtAlCl_2$ was again found to effectively promote the key ring rearrangement to complete the C/D ring system. The resulting ketone (**31**) was subjected to excess $LiAlH_4$ to reduce the C6 carbonyl and remove two benzoyl protecting groups simultaneously. The crude product of hexol **32** underwent selective cleavage of the less sterically hindered 1,2-diol to furnish hemiketal **33** in 69% yield over two steps.

The assignment of the stereochemistry of **33** by NOESY experiment (see SI) set the stage for the inversion of the C1 and C6 stereogenic centers. Protection of **33** using acetonide followed by Dess−Martin periodinane (DMP) oxidation was executed in a one-pot fashion to furnish acetonide **34** in 66% yield. By carefully optimizing the reduction/deprotection sequence and reaction conditions (Table S2), we first used DIBAL-H to regio- and diastereoselectively reduce the C1 ketone under −100 °C in DCM/ether (3:1), followed by addition of Red-Al to reduce the C6 carbonyl group, which provided diastereomeric (−)-**35** and (−)-**3** in 21% and 56% isolated yield, respectively, after in situ deprotection. The undesired product (**35**) could be readily recycled to **34** via

DOI: 10.1021/jacs.9b12034
J. Am. Chem. Soc. 2019, 141, 20048−20052

protection and oxidation. The singlet oxygen ene reaction of **3** followed by trichloroisocyanuric acid (TCCA) treatment forged the enone motif,[9c] but (−)-oridonin (**2**) was obtained in low and unstable yield (see SI). Eventually, we found $(Boc)_2O$ could efficiently convert the allylic hydroperoxide derived from (−)-**3** into enone, but the C14 hydroxyl group was also protected concomitantly. Therefore, the addition of HCl ensued, and this one-pot operation resulted in the isolation of **2** in 47% yield. All of the analytic data for the synthesized sample of **2** were consistent with those reported in the literature (Table S3).[25]

In summary, the first total synthesis of (−)-oridonin (**2**) was achieved with a route flexibly adhering to our original plan proposed in Figure 1. The stereochemical relationship of the continuous stereogenic centers, although challenging, served as a source of inspiration for an innovative strategy toward *ent*-kaurene diterpenoids. This work further demonstrated the power of the interrupted Nazarov cyclization in the context of total synthesis. The other highlight of our strategy was the critical skeletal rearrangement via two 1,2-migration transformations. Furthermore, two synthons, (+)-**9** and (+)-**10**, accessed by robust and scalable synthetic routes, could be extended for the synthesis of other terpenoids. This work is under way and will be reported in due course.

■ ASSOCIATED CONTENT

Supporting Information

The Supporting Information is available free of charge at https://pubs.acs.org/doi/10.1021/jacs.9b12034.

Experimental procedures and spectral data for all new compounds (PDF)
X-ray crystallographic data for **11** (CIF)
X-ray crystallographic data for **S3** (CIF)
X-ray crystallographic data for **S4** (CIF)
X-ray crystallographic data for **26** (CIF)
X-ray crystallographic data for **28** (CIF)

■ AUTHOR INFORMATION

Corresponding Author

*tuopingluo@pku.edu.cn

ORCID

Tuoping Luo: 0000-0003-2156-3198

Author Contributions

§L. Kong and F. Su contributed equally.

Notes

The authors declare no competing financial interest.

■ ACKNOWLEDGMENTS

This work was supported by College of Chemistry and Molecular Engineering, Peking University, and Peking-Tsinghua Center for Life Sciences, Beijing National Laboratory for Molecular Sciences, the National Science Foundation of China (Grant Nos. 31521004, 21672011, and 21822101), and National Key Research and Development Program of China (Grant No. 2017YFA0104003). The measurements of NMR, mass spectrometry, and XRD were performed at the Analytical Instrumentation Center of Peking University. We acknowledge the assistance and support from PKUAIC (Dr. Jie Su) and support from the High-Performance Computing Platform of Peking University. Dedicated to Professor Zhen Yang on the occasion of his 60th birthday.

■ REFERENCES

(1) Liu, M.; Wang, W. G.; Sun, H.-D.; Pu, J.-X. Diterpenoids from Isodon species: an update. *Nat. Prod. Rep.* **2017**, *23*, 673−698.

(2) (a) Fujita, E.; Fujita, T.; Katayama, H.; Shibuya, M. Oridonin, a new diterpenoid from Isodon species. *Chem. Commun.* **1967**, 252−254. (b) Xu, J.; Wold, E. A.; Ding, Y.; Shen, Q.; Zhou, J. Therapeutic potential of oridonin and its analogs: from anticancer and antiinflammation to neuroprotection. *Molecules* **2018**, *23*, 474.

(3) (a) Li, D.; Xu, S.; Cai, H.; Pei, L.; Zhang, H.; Wang, L.; Yao, H.; Wu, X.; Jiang, J.; Sun, Y.; Xu, J. Enmein-type diterpenoid analogs from natural kaurene-type oridonin: synthesis and their antitumor biological evaluation. *Eur. J. Med. Chem.* **2013**, *64*, 215−221. (b) Ding, C.; Zhang, Y.; Chen, H.; Yang, Z.; Wild, C.; Chu, L.; Liu, H.; Shen, Q.; Zhou, J. Novel nitrogen-enriched oridonin analogues with thiazole-fused A-ring: protecting group-free synthesis, enhanced anticancer profile, and improved aqueous solubility. *J. Med. Chem.* **2013**, *56*, 5048−5058. (c) Ding, C.; Zhang, Y.; Chen, H.; Yang, Z.; Wild, C.; Ye, N.; Ester, C. D.; Xiong, A.; White, M. A.; Shen, Q.; Zhou, J. Oridonin ring A-based diverse constructions of enone functionality: identification of novel dienone analogues effective for highly aggressive breast cancer by inducing apoptosis. *J. Med. Chem.* **2013**, *56*, 8814−8825. (d) Xu, S.; Yao, H.; Luo, S.; Zhang, Y. K.; Yang, D. H.; Li, D.; Wang, G.; Hu, M.; Qiu, Y.; Wu, X.; Yao, H.; Xie, W.; Chen, Z. S.; Xu, J. A novel potent anticancer compound optimized from a natural oridonin scaffold induces apoptosis and cell cycle arrest through the mitochondrial pathway. *J. Med. Chem.* **2017**, *60*, 1449−1468. (e) Ding, Y.; Li, D.; Ding, C.; Wang, P.; Liu, Z.; Wold, E. A.; Ye, N.; Chen, H.; White, M. A.; Shen, Q.; Zhou, J. Regio- and stereospecific synthesis of oridonin D-ring aziridinated analogues for the treatment of triple-negative breast cancer via mediated irreversible covalent warheads. *J. Med. Chem.* **2018**, *61*, 2737−2752. (f) Luo, D.; Yi, Y.; Peng, K.; Liu, T.; Yang, J.; Liu, S.; Zhao, W.; Qu, X.; Yu, W.; Gu, Y.; Wan, S. Oridonin derivatives as potential anticancer drug candidates triggering apoptosis through mitochondrial pathway in the liver cancer cells. *Eur. J. Med. Chem.* **2019**, *178*, 365−379.

(4) CTR20150246; http://www.chinadrugtrials.org.cn/, accessed on June 27, 2019.

(5) (a) Xu, Y.; Xue, Y.; Wang, Y.; Feng, D.; Lin, S.; Xu, L. Multiple-modulation effects of oridonin on the production of proinflammatory cytokines and neurotrophic factors in LPS-activated microglia. *Int. Immunopharmacol.* **2009**, *9*, 360−365. (b) Zhang, Z. Y.; Daniels, R.; Schluesener, H. J. Oridonin ameliorates neuropathological changes and behavioural deficits in a mouse model of cerebral amyloidosis. *J. Cell. Mol. Med.* **2013**, *17*, 1566−1576. (c) Wang, S.; Yang, H.; Yu, L.; Jin, J.; Qian, L.; Zhao, H.; Xu, Y.; Zhu, X. Oridonin attenuates Aβ_{1-42}-induced neuroinflammation and inhibits NF-κB pathway. *PLoS One* **2014**, *9*, e104745. (d) Wang, S.; Yu, L.; Yang, H.; Li, C.; Hui, Z.; Xu, Y.; Zhu, X. Oridonin attenuates synaptic loss and cognitive deficits in an Aβ_{1-42}-induced mouse model of Alzheimer's disease. *PLoS One* **2016**, *11*, e0151397.

(6) (a) Zhen, T.; Wu, C. F.; Liu, P.; Wu, H. Y.; Zhou, G. B.; Lu, Y.; Liu, J. X.; Liang, Y.; Li, K. K.; Wang, Y. Y.; Xie, Y. Y.; He, M. M.; Cao, H. M.; Zhang, W. N.; Chen, L. M.; Petrie, K.; Chen, S. J.; Chen, Z. Targeting of AML1-ETO in t(8;21) leukemia by oridonin generates a tumor suppressor-like protein. *Sci. Transl. Med.* **2012**, *4*, 127ra38. (b) Owona, B. A.; Schluesener, H. J. Molecular insight in the multifunctional effects of oridonin. *Drugs R&D* **2015**, *15*, 233−244. (c) Dal Piaz, F.; Cotugno, R.; Lepore, L.; Vassallo, A.; Malafronte, N.; Lauro, G.; Bifulco, G.; Belisario, M. A.; De Tommasi, N. Chemical proteomics reveals HSP70 1A as a target for the anticancer diterpene oridonin in Jurkat cells. *J. Proteomics* **2013**, *82*, 14−26. (d) Vasaturo, M.; Cotugno, R.; Fiengo, L.; Vinegoni, C.; Dal Piaz, F.; De Tommasi, N. The anti-tumor diterpene oridonin is a direct inhibitor of Nucleolin in cancer cells. *Sci. Rep.* **2018**, *8*, 16735. (e) He, H.; Jiang, H.; Chen, Y.; Ye, J.; Wang, A.; Wang, C.; Liu, Q.; Liang, G.; Deng, X.; Jiang, W.; Zhou, R. Oridonin is a covalent NLRP3 inhibitor with strong anti-inflammasome activity. *Nat. Commun.* **2018**, *9*, 2550.

DOI: 10.1021/jacs.9b12034
J. Am. Chem. Soc. 2019, 141, 20048−20052

(7) Zhou, W.-S.; Cheng, Y.-X. The stereo-, regio-, and chemoselective conversion of diterpenoids, kamebakaurin to oriaonin. *Sci. China Ser. B-Chem.* **1992**, *35*, 194−199.
(8) For reviews of *ent*-kauranoid total synthesis, see: (a) Lazarski, K. E.; Moritz, B. J.; Thomson, R. J. The total synthesis of *Isodon* diterpenes. *Angew. Chem., Int. Ed.* **2014**, *53*, 10588−10599. (b) Riehl, P. S.; DePorre, Y. C.; Armaly, A. M.; Groso, E. J.; Schindler, C. S. New avenues for the synthesis of *ent*-kaurene diterpenoids. *Tetrahedron* **2015**, *71*, 6629−6650.
(9) For syntheses of highly oxidized *ent*-kauranoids with an intact *ent*-kaurene carbon skeleton, see: (a) Yeoman, J. T. S.; Mark, V. W.; Reisman, S. E. A unified strategy to *ent*-kauranoid natural products: total syntheses of (−)-trichorabdal A and (−)-longikaurin E. *J. Am. Chem. Soc.* **2013**, *135*, 11764−11767. (b) Zhao, X.; Li, W.; Wang, J.; Ma, D. Convergent route to *ent*-kaurane diterpenoids: total synthesis of lungshengenin D and 1α,6α-diacetoxy-*ent*-kaura-9(11),16-dien-12,15-dione. *J. Am. Chem. Soc.* **2017**, *139*, 2932−2935. (c) He, C.; Hu, J.; Wu, Y.; Ding, H. Total syntheses of highly oxidized *ent*-kaurenoids pharicin A, pharicinin B, 7-*O*-acetylpseurata C, and pseurata C: a [5 + 2] cascade approach. *J. Am. Chem. Soc.* **2017**, *139*, 6098−6101. (d) Su, F.; Lu, Y.; Kong, L.; Liu, J.; Luo, T. Total synthesis of maoecrystal P: application of a strained bicyclic synthon. *Angew. Chem., Int. Ed.* **2018**, *57*, 760−764. (e) Zhu, L.; Ma, W.; Zhang, M.; Lee, M. M.-L.; Wong, W.-Y.; Chan, B. D.; Yang, Q.; Wong, W.-T.; Tai, W. C.-S.; Lee, C.-S. Scalable synthesis enabling multilevel bio-evaluations of natural products for discovery of lead compounds. *Nat. Commun.* **2018**, *9*, 1283.
(10) For syntheses of highly oxidized *ent*-kauranoids with a rearranged or cleaved *ent*-kaurene skeleton, see: (a) Gong, J.; Lin, G.; Sun, W.; Li, C.-C.; Yang, Z. Total synthesis of (±) maoecrystal V. *J. Am. Chem. Soc.* **2010**, *132*, 16745−16746. (b) Cha, J. Y.; Yeoman, J. T. S.; Reisman, S. E. A concise total synthesis of (−)-maoecrystal Z. *J. Am. Chem. Soc.* **2011**, *133*, 14964−14967. (c) Peng, F.; Danishefsky, S. J. Total synthesis of (±) maoecrystal V. *J. Am. Chem. Soc.* **2012**, *134*, 18860−18867. (d) Lu, P.; Gu, Z.; Zakarian, A. Total synthesis of maoecrystal V: early-stage C−H functionalization and lactone assembly by radical cyclization. *J. Am. Chem. Soc.* **2013**, *135*, 14552−14555. (e) Lu, P.; Mailyan, A.; Gu, Z.; Guptill, D. M.; Wang, H.; Davies, H. M. L.; Zakarian, A. Enantioselective synthesis of (−)-maoecrystal V by enantiodetermining C−H functionalization. *J. Am. Chem. Soc.* **2014**, *136*, 17738−17749. (f) Zheng, C.; Dubovyk, I.; Lazarski, K. E.; Thomson, R. J. Enantioselective total synthesis of (−)-maoecrystal V. *J. Am. Chem. Soc.* **2014**, *136*, 17750−17756. (g) Moritz, B. J.; Mack, D. J.; Tong, L.; Thomson, R. J. Total synthesis of the *Isodon* diterpene sculponeatin N. *Angew. Chem., Int. Ed.* **2014**, *53*, 2988−2991. (h) Pan, Z.; Zheng, C.; Wang, H.; Chen, Y.; Li, Y.; Cheng, B.; Zhai, H. Total synthesis of (±)-sculponeatin N. *Org. Lett.* **2014**, *16*, 216−219. (i) Cernijenko, A.; Risgaard, R.; Baran, P. S. 11-Step total synthesis of (−)-maoecrystal V. *J. Am. Chem. Soc.* **2016**, *138*, 9425−9428. (j) Lv, Z.; Chen, B.; Zhang, C.; Liang, G. Total syntheses of trichorabdal A and maoecrystal Z. *Chem. - Eur. J.* **2018**, *24*, 9773−9777. (k) Wu, J.; Kadonaga, Y.; Hong, B.; Wang, J.; Lei, X. Enantioselective total synthesis of (+)-jungermatrobrunin A. *Angew. Chem., Int. Ed.* **2019**, *58*, 10879−10883. (l) Zhang, J.; Li, Z.; Zhuo, J.; Cui, Y.; Han, T.; Li, C. Tandem decarboxylative cyclization/alkenylation strategy for total syntheses of (+)-longirabdiol, (−)-longirabdolactone, and (−)-effusin. *J. Am. Chem. Soc.* **2019**, *141*, 8372−8380.
(11) (a) Fraga, B. M.; Hanson, J. R.; Hernández, M. G.; Tellado, F. G. The first partial synthesis of 14-hydroxy-gibberellin esters. A titanium(IV)-amide catalyzed rearrangement of epoxides. *Tetrahedron Lett.* **1989**, *30*, 6899−6902. (b) Dueñas, J.; García-Granados, A.; Martínez, A.; Onorato, E.; Parra, A. Opening of ring C in ruthenium-catalyzed rearrangements of 15,16-epoxybeyerane diterpenes hydroxylated at C-12. *J. Org. Chem.* **1995**, *60*, 2170−2173.
(12) Benjamin, L. J.; Mander, L. N.; Willis, A. C. Conversion of a gibberellin aldehyde into a 20-norkaurenoid lactone. *Tetrahedron Lett.* **1996**, *37*, 8937−8940.
(13) For reviews of the interrupted Nazarov reactions, see: (a) Grant, T. N.; Rieder, C. J.; West, F. G. Interrupting the Nazarov reaction: domino and cascade processes utilizing cyclopentenyl cations. *Chem. Commun.* **2009**, 5676−5688. (b) Shirinian, V. Z.; Yadykov, A. Recent advances in the interrupted Nazarov reaction. *Adv. Synth. Catal.* **2019**, DOI: 10.1002/adsc.201901001.
(14) (a) Giese, S.; Kastrup, L.; Stiens, D.; West, F. G. Intermolecular trapping of the Nazarov intermediate: domino electrocyclization/[3 + 2] cycloadditions with allylsilanes. *Angew. Chem., Int. Ed.* **2000**, *39*, 1970−1973. (b) Kwon, Y.; McDonald, R.; West, F. G. Organoaluminum-mediated interrupted Nazarov reaction. *Angew. Chem., Int. Ed.* **2013**, *52*, 8616−8619. (c) Wu, Y.-K.; Dunbar, C. R.; McDonald, R.; Ferguson, M. J.; West, F. G. Experimental and computational studies on interrupted Nazarov reactions: exploration of umpolung reactivity at the α-carbon of cyclopentanones. *J. Am. Chem. Soc.* **2014**, *136*, 14903−14911. (d) Yadav, V. K.; Naganaboina, V. K.; Hulikal, V. Allylsilane-interrupted homo-Nazarov cyclization and synthesis of bicyclo[3.2.1]octan-8-ones. *Tetrahedron Lett.* **2014**, *55*, 2015−2018.
(15) For use of PBr_3 in the Vilsmeier reaction, see: Huang, A. X.; Xiong, Z.; Corey, E. J. An exceptionally short and simple enantioselective total synthesis of pentacyclic triterpenes of the β-amyrin family. *J. Am. Chem. Soc.* **1999**, *121*, 9999−10003.
(16) Lang, G. L.; Decicco, C. D.; Willson, J.; Strickland, L. A. Ring expansions of [2 + 2] photoadducts. Potential applications in the synthesis of triquinane and taxane skeletons. *J. Org. Chem.* **1989**, *54*, 1805−1810.
(17) Corey, E. J.; Helal, C. J. Reduction of carbonyl compounds with chiral oxazaborolidine catalysts: a new paradigm for enantioselective catalysis and a powerful new synthetic method. *Angew. Chem., Int. Ed.* **1998**, *37*, 1986−2012.
(18) May, T. L.; Dabrowski, J. A.; Hoveyda, A. H. Formation of vinyl-, vinylhalide- or acyl-substituted quaternary carbon stereogenic centers through NHC-Cu-catalyzed enantioselective conjugate additions of Si-containing vinylaluminums to β-substituted cyclic enones. *J. Am. Chem. Soc.* **2011**, *133*, 736−739.
(19) Hein, S. J.; Arslan, H.; Keresztes, I.; Dichtel, W. R. Rapid synthesis of crowded aromatic architectures from silyl acetylenes. *Org. Lett.* **2014**, *16*, 4416−4419.
(20) Duchene, A.; Abarbri, M.; Parrain, J. L.; Kitamura, M.; Noyori, R. Synthesis of 3-substituted but-3-enoic acids via palladium catalysed cross-coupling reaction of 3-iodobut-3-enoic acid with organometallic reagents. *Synlett* **1994**, *1994*, 524−526.
(21) Mihelich, E. D.; Eickhoff, D. J. A one-pot conversion of olefins to α,β-unsaturated carbonyl compounds. An easy synthesis of 2-cyclopentenone and related compounds. *J. Org. Chem.* **1983**, *48*, 4135−4137.
(22) Ohno, K.; Tsuji, J. Organic synthesis by means of noble metal compounds. XXXV. Novel decarbonylation reactions of aldehydes and acyl halides using rhodium complexes. *J. Am. Chem. Soc.* **1968**, *90*, 99−107.
(23) Wang, B. M.; Song, Z. L.; Fan, C. A.; Tu, Y. Q.; Chen, W. M. Halogen cation induced stereoselective semipinacol-type rearrangement of allylic alcohols. A highly efficient approach to α-quaternary β-haloketo compounds. *Synlett* **2003**, 1497−1499.
(24) Carlsen, P. H. J.; Katsuki, T.; Martin, V. S.; Sharpless, K. B. A greatly improved procedure for ruthenium tetroxide catalyzed oxidations of organic compounds. *J. Org. Chem.* **1981**, *46*, 3936−3938.
(25) (a) Fujita, E.; Fujita, T.; Katayama, H.; Shibuya, M.; Shingu, T. Terpenoids. Part XV. Structure and absolute configuration of oridonin isolated from *Isodon japonicus* and *Isodon trichocarpus*. *J. Chem. Soc. C* **1970**, 1674−1681. (b) Lu, Y.; Sun, C.; Pan, Y. Isolation and purification of oridonin from *Rabdosia rubescens* using upright counter-current chromatography. *J. Sep. Sci.* **2006**, *29*, 314−318.

DOI: 10.1021/jacs.9b12034
J. Am. Chem. Soc. 2019, 141, 20048−20052